The BRCA1-11q Alternative Splice Isoform Bypasses Germline Mutations and Promotes Therapeutic Resistance to PARP Inhibition and Cisplatin.

The BRCA1-Δ11q Alternative Splice Isoform Bypasses Germline Mutations and Promotes Therapeutic Resistance to PARP Inhibition and Cisplatin

Yifan Wang[1,28], Andrea J. Bernhardy[1,28], Cristina Cruz[2,3], John J. Krais[1], Joseph Nacson[1], Emmanuelle Nicolas[4], Suraj Peri[1], Hanneke van der Gulden[5], Ingrid van der Heijden[5], Shane W. O'Brien[1], Yong Zhang[6], Maribel I. Harrell[7], Shawn F. Johnson[8], Francisco J. Candido Dos Reis[9,10], Paul D. P. Pharoah[10], Beth Karlan[11], Charlie Gourley[12], Diether Lambrechts[13], Georgia Chenevix-Trench[14], Håkan Olsson[15], Javier J. Benitez[16], Mark H. Greene[17], Martin Gore[18], Robert Nussbaum[19], Siegal Sadetzki[20], Simon A. Gayther[21], Susanne K. Kjaer[22], kConFab Investigators[23], Alan D. D'Andrea[24, 25], Geoffrey I. Shapiro[8, 26], David L. Wiest[6], Denise C. Connolly[1], Mary B. Daly[27], Elizabeth M. Swisher[7], Peter Bouwman[5], Jos Jonkers[5], Judith Balmaña[2], Violeta Serra[3] and Neil Johnson[1*]

[1] Molecular Therapeutics Program, [4] Cancer Biology Program, [6] Immune Cell Development and Host Defense Program, [27]Risk Assessment Program, Fox Chase Cancer Center, Philadelphia, Pennsylvania, USA
[2]High Risk and Cancer Prevention Group, [3]Experimental Therapeutics Group, Vall d'Hebron Institute of Oncology, Barcelona, Spain
[5]Division of Pathology, The Netherlands Cancer Institute, Amsterdam, the Netherlands
[7]Department of Obstetrics and Gynecology and Medicine, University of Washington, Seattle, Washington, USA
[8]Department of Medical Oncology, [24]Department of Radiation Oncology, Dana-Farber Cancer Institute and Harvard Medical School, Boston, Massachusetts, USA
[9]Department of Gynecology and Obstetrics, Ribeirao Preto Medical School, University of Sao Paulo, Sao Paulo, Brazil
[10]Centre for Cancer Genetic Epidemiology, University of Cambridge, UK
[11]Women's Cancer Program at the Samuel Oschin Comprehensive Cancer Institute, Cedars-Sinai Medical Center, Los Angeles, CA, USA
[12]University of Edinburgh Cancer Research UK Centre, MRC IGMM, UK
[13]VIB Vesalius Research Center, University of Leuven, Leuven, Belgium
[14]QIMR Berghofer Medical Research Institute, Herston, Australia
[15]Departments of Cancer Epidemiology and Oncology, Lund University, Lund, Sweden
[16]Human Genetics Group and Human Genotyping Unit Spanish National Cancer Research Centre (CNIO), Madrid, Spain
[17]Division of Cancer Epidemiology and Genetics, National Cancer Institute, Rockville, MD, USA
[18]Royal Marsden NHS Foundation Trust, UK
[19]University of California San Francisco, Cancer Risk Program, San Francisco, CA, USA
[20]Gertner Institute for Epidemiology and Health Policy Research, Sheba Medical Center, Tel Hashomer, Israel

[21]Department of Preventive Medicine, Keck School of Medicine, University of Southern California Norris Comprehensive Cancer Center, Los Angeles, CA, USA
[22]Department of Virus, Lifestyle and Genes, Danish Cancer Society Research Center, Copenhagen, Denmark
[23]University of Melbourne, Melbourne, Australia
[25]Department of Pediatrics, Children's Hospital and Harvard Medical School, Boston, Massachusetts, USA
[26]Department of Medicine, Brigham and Women's Hospital and Harvard Medical School, Boston, Massachusetts, USA

[28]Co-first author
*Correspondence: neil.johnson@fccc.edu

Contact: Neil Johnson, Molecular Therapeutics Program, Fox Chase Cancer Center, Philadelphia, Pennsylvania, 19111, USA. Phone: 215-728-7016; Fax: 215-728-2741; E-mail: neil.johnson@fccc.edu

The authors declare no conflicts of interest.

Abstract

Breast and ovarian cancer patients harboring *BRCA1/2* germline mutations have clinically benefitted from therapy with PARP inhibitor (PARPi) or platinum compounds, but acquired resistance limits clinical impact. In this study, we investigated the impact of mutations on *BRCA1* isoform expression and therapeutic response. Cancer cell lines and tumors harboring mutations in exon 11 of *BRCA1* express a *BRCA1-Δ11q* splice variant lacking the majority of exon 11. The introduction of frameshift mutations to exon 11 resulted in nonsense-mediated mRNA decay of full-length, but not the *BRCA1-Δ11q* isoform. CRISPR/Cas9 gene editing as well as overexpression experiments revealed that the BRCA1-Δ11q protein was capable of promoting partial PARPi and cisplatin resistance relative to full-length BRCA1, both *in vitro* and *in vivo*. Furthermore, spliceosome inhibitors reduced BRCA1-Δ11q levels and sensitized cells carrying exon 11 mutations to PARPi treatment. Taken together, our results provided evidence that cancer cells employ a strategy to remove deleterious germline *BRCA1* mutations through alternative mRNA splicing, giving rise to isoforms that retain residual activity and contribute to therapeutic resistance.

Introduction

Germline mutations in the *BRCA1* gene are associated with an increased risk of developing breast and ovarian cancer (1, 2). Mutations often result in reading frameshifts and nonsense-mediated mRNA decay (NMD) (3). The BRCA1 protein is essential for efficient homologous recombination (HR) mediated repair of double stranded DNA breaks (4, 5). Inhibitors of poly(ADP-ribose) polymerase (PARP), as well as platinum agents, induce double stranded DNA breaks that are can be repaired by the HR DNA repair pathway (6, 7). Consequently, cells that have defective HR DNA repair, such as those with dysfunctional BRCA1 or BRCA2 proteins are highly sensitive to PARP inhibitor (PARPi) or platinum treatments (8-11).

Although PARP inhibitors have been shown to provide survival improvements, many patients that harbor germline *BRCA1* or *BRCA2* mutations do not gain benefit from PARPi therapy (12-14). Additionally, many patients that first benefit from either PARPi or platinum therapy develop disease progression and resistance (15). PARPi or platinum resistance has been demonstrated to arise by a variety of mechanisms, including reversion mutations (16, 17), loss of 53BP1 pathway activity(18, 19), expression of hypomorphic BRCA1 proteins (20, 21), and drug efflux (22).

BRCA1 mRNA isoforms generated by alternative splicing lack specific exons and have been show to be expressed in cells and tissues (23-25). In particular, the relative levels of *BRCA1* exon 11 splice isoforms differ between normal and cancer tissues and in discrete phases of the cell cycle (26-29). These isoforms include *BRCA1* full-length (inclusion of

all coding exons), Δ11 (skipping of exon 11) and Δ11q (partial skipping of exon 11). The *BRCA1-Δ11q* isoform derives from use of an alternative exon 11 splice donor site, resulting in the exclusion of most exon 11 nucleotides (c.788-4096) (Supplementary Fig. S1) (27, 28). In human cells and tissues, the *BRCA1- Δ11q* isoform expression is more readily detectable than the *BRCA1-Δ11* isoform (26, 29, 30).

The BRCA1-Δ11 isoform has previously been implicated in both cell death and proliferation in mouse studies. Both *Brca1*-null and $Brca1^{\Delta 11/\Delta 11}$ mice that exclusively express Brca1-Δ11 undergo embryonic lethality, but $Brca1^{\Delta 11/\Delta 11}$ embryos die at a later stage, suggesting that Brca1-Δ11 isoform can partially compensate for the lack of other Brca1 isoforms during embryogenesis (31-33). *BRCA1* mutations located in exon 11 represent approximately 30% of the overall number of mutation carriers that develop breast and ovarian cancer in the US (34-37). Here, we examined the impact of exon 11 mutations on *BRCA1* isoform expression and therapy response.

Methods

Cell lines and reagents

Cells were purchased from Asterand or ATCC. Cycloheximide, actinomycin D, puromycin, blastcitidine, DMSO were purchased from Sigma-Aldrich, cisplatin was from APP/Fresenius Kabai USA LLC and placlitaxel from Sagent Pharmaceuticals. Pladienolide B (Pl-B) was purchased from Calbiochem. Clovis provided rucaparib (CO-338) and olaparib (AZD2281) was purchased from Selleckchem. BRCA1 mutated cell

lines were validated through DNA sequencing and the identification of specific BRCA1 mutations that are uniquely present in individual cell lines as well as DNA fingerprinting. Cell lines tested negative for mycoplasma.

Colony formation assays

Depending on colony forming potential, cells were seeded at a density ranging from 500 – 4000 cells per well in 6 well plates in the presence of increasing concentrations of either rucaparib or olaparib. For cisplatin and taxol treatments, exponentially growing cells were cultured in 24 well plates, treated with increasing concentrations of cisplatin and taxol for 24 hours and replated in 6 well plates for colony formation. For shRNA or cDNA add back colony formation experiments, cells were treated as for above, but with the addition of either puromycin or blastcitidine in the media. For siRNA treatments, exponentially growing cells were reverse transfected in 24 well plates, 2 days post transfection cells were treated with rucaparib for 72 hours and then replated in 6 well plates for colony formation. For Pladienolide B colony assays, cells were treated with Pladienolide B (1.25 nM) and rucaparib (100 nM) for 72 hours and then replated into 6 well plates for colony formation. Colony formation was assessed 2 weeks post plating with crystal violet staining. Mean colony formation from three experiments was expressed as percentage of colonies $\pm$ S.E. relative to vehicle-treated cells.

Gene sequencing RT-PCR analysis

Genomic DNA was isolated from cells using the DNeasy tissue kit (Qiagen). To determine if gene rearrangements had taken place that would have excluded the exon 11q

region from genomic DNA of cell lines and PDX tumors, we carried out PCR using OneTaq Hot Start 2X Master Mix (NEB) and gDNA as templates. Primers were located in exon 10 (Forward) and 12 (Reverse): F:aatcacccctcaaggaacca; R:ctcacacccagatgctgcttc. Total RNA was isolated from cell lines using RNAeasy kit (Qiagen). For Quantitative RT-PCR, RNA was tested for quality on a Bioanalyzer (Agilent). RNA concentrations were determined with a spectrophotometer (NanoDrop; Thermo Fisher Scientific). RNA was reverse transcribed using Moloney murine leukemia virus reverse transcriptase (Ambion) and a mixture of anchored oligo-dT and random decamers. Two reverse-transcription reactions were performed for each sample using either 100 or 25 ng of input RNA. Assays were used in combination with Taqman Universal Master mix or Power SybrGreen master mix and run on a 7900 HT sequence detection system (Applied Biosystems). Cycling conditions were 95°C, 15 min, followed by 40 (two-step) cycles (95°C, 15 s; 60°C, 60 s). Ct (cycle threshold) values were converted to quantities (in arbitrary units) using a standard curve (four points, four fold dilutions) established with a calibrator sample. For each sample, the values are averaged and S.D. of data derived from two independent PCRs. For the BRCA1 splice variants, amplicons quantified by on-chip electrophoresis on an Agilent 2100 Bioanalyzer were used for absolute quantification assays. Primers that specifically recognize the following BRCA1 mRNA isoforms were used: exon +11 containing: F:tagcaaggagccaacataacagat; R:cttattccattcttttctctcacacag; Δ11q: F:gattctgcaaaaaaggctgct; R:cagatgctgcttcaccctga For RBFOX2 F:aagcccagtagttggagctgt, R:ttgcctagggacacatctgctt; and POLR2F: F:tgccatgaaggaactcaagg R: tcatagctcccatctggcag. BRCA1 expression values were routinely normalized to a *POL2RF* house keeping gene (HKG) control and expressed as a

percentage of the values calculated for MDA-MB-231 cells or to a relevant control sample.

BRCA1-minigene generation and analysis

Genomic DNA derived from blood lymphocytes of healthy individuals was tested for the absence of mutations by BROCA sequencing. The entire genomic region of BRCA1 from exon 8 to exon 12 was amplified with the following 5 PCR reactions and primer sets:

1F: ccgctcgagAACCTTGGAACTGTGAGAACTCTG

1R: ccggatatCAATTTGAGAGCCCAGTTTGAAT

2F: ccgctcgagAACCTGGGTGACAGAGCAAGA

2R: ccggatatcAGGGAAAAGACAGAGTCCTAATAAGA

3F: ccgctcgagAGAGCTAAAATGTTTGATCTTGGTC

3R: ccggatatcTCTTGATAAAATCCTCAGGATGAAG

4F: ccgctcgagATTTGGGAAAACCTATCGGAAG

4R: ccggatatcTAATACTGGAGCCCACTTCATTAGT

5F: ccgctcgagCCAGCTCAAGCAATATTAATGAAGT

5R: ccggatatcGTTAAAATGTCACTCTGAGAGGATAGC

HA-tag was cloned into pENTRA vector using SalI and XhoI sites. Each BRCA1 fragment was first cloned into pENTRA-HA vector using XhoI (shown in lowercase forward primers above) and EcoRV (shown in lowercase reverse primers above) sites. The 5 cloned fragments were assembled into a minigene using the following restriction sites that corresponded with cut sites in each fragment: EcoRI, SpeI, StuI and ScaI sites. An eGFP fragment was cloned into the 3'end of the exon 12 fragment using EcoRV site.

The minigene was then shuttled into pcDNA6.2 Destination vector using the LR Clonase system (Invitrogen). We confirmed by Sanger sequencing that mutations were not introduced into exons or introns within 500 bp flanking each exon. The indicated mutations (see Supplementary Fig. 3a) were introduced using site directed mutagenesis (Agilent) using the following primers:

2288delT F: ccagtgaacttaaagaatttgtcaacctagccttccaaga

2288delT R: tcttggaaggctaggttgacaaattctttaagttcactgg

2529C>T F: caaatgctgcacactaactcacacatttatttggttctgtttttg

2529C>T R: caaaaacagaaccaaataaatgtgtgagttagtgtgcagcatttg

3960C>T F：ctaaggtgatgttcctaagatgcctttgccaatattacc

3960C>T R：ggtaatattggcaaaggcatcttaggaacatcaccttag

1stFOXMut F: tcagggtagttctgtttcaaacttacacgtggagccatgtg

1stFOXMut R: cacatggctccacgtgtaagtttgaaacagaactaccctga

2ndFOXMut F:gagtaataaactgctgttctcgtgttgtaatgagctggcatgagta

2ndFOXMut R: tactcatgccagctcattacaacacgagaacagcagtttattactc

Ex11qsplice F: tgcaagtttgaaacagaactcccctgatactttctggatg

Ex11qsplice R: catccagaaaagtatcaggggagttctgtttcaaacttgca

To measure *BRCA1-Δ11q*-reporter expression total RNA was isolated from transfected using RNAeasy kit (Qiagen). cDNA was synthesized using High-Capacity cDNA Reverse Transcription Kit (Applied Biosystems). PCR was performed using OneTaq Hot Start 2X Master Mix (NEB). Primers that specifically recognize *BRCA1-Δ11q*-reporter mRNA: F: gattctgcaaaaaaggctgct; R: agtcgtgctgcttcatgtggt; and *BSD*: F:

gcctttgtctcaagaagaatcca; R: tagccctcccacacataacca. Additionally, Western blots using HA antibody detected BRCA1-Δ11q-reporter protein expression.

Western blotting

Western blotting was carried out as previously described and proteins detected using the following antibodies: BRCA1: N-terminal: (MS110, EMD), C-terminal: (D9, Santa Cruz Biotechnology), BRCA1 (9010, Cell Signaling), Tubulin (2148, Cell Signaling), HA (23675, Cell Signaling), RAD51 (H-92, Santa Cruz Biotechnology), Pol II (C-18, (Santa Cruz Biotechnology), CtIP (A300-438-A, Bethyl Labs), PALB2 (A301-247A1, Bethyl Labs), BARD1 (A300-263A, Bethyl Labs), BRCA2 (OP-95, EMD). HA (23675, Cell Signaling) antibody was used for immunoprecipitation of HA-BRCA1 complexes from 2 mg of nuclear extract using Pierce Classic IP Kit (Thermo Scientific) according to the manufacturer's instructions. Nuclear extracts were derived using NE-PER Nuclear and Cytoplasmic Extraction Reagents (Thermo Scientific) according to the manufacturer's instructions. Densitometric analyses were carried out using Image J.

Immunofluorescence and microscopy

For immunofluorescence HA (HA.11, Covance), BRCA1 (MS110, EMD), γ-H2AX [pS139] (N1-4131, EMD) and RAD51 (H-92, Santa Cruz Biotechnology), geminin (10802-1-AP, ProteinTech Group) and geminin (Abnova, E7071-1A8) antibodies were followed by secondary antibodies conjugated to FITC or Texas Red (Jackson ImmunoResearch Laboratories). We acquired immunofluorescence images using Nikon

NIU Upright Fluorescent Microscope and generated images using Nikon NIS Elements software. For IR experiments, we routinely fixed cells 8 hours after treatment with 10 Gy. For analyses, we counted a minimum of 200 cells per condition or cell line. Foci positive cells were expressed as a percentage of geminin positive cells to account for any differences in S/G2/M populations between cell lines. Each experiment was carried out three times with biological replicates. γ-H2AX IRIF was present equally in all cell lines and routinely measured as a positive control for IRIF.

Immunofluorescence and immunohistochemical analyses of tumors

For BRCA1 focus formation analysis, tissue sections were deparaffinized with xylene and hydrated with decreasing concentrations of ethanol. For target antigen retrieval, sections were microwaved in DAKO Antigen Retrieval Buffer pH 9.0 for 4 minutes at 110ºC (a T/T MEGA multifunctional Microwave Histoprocessor (Milestone)). Sections were cooled down in distilled water for 5 minutes, then permeabilized with DAKO Wash Buffer containing Tween 20 for 5 minutes, followed by incubation in blocking buffer (DAKO Wash Buffer with 1% BSA) for 5 minutes. Primary antibodies were diluted in DAKO Antibody Diluent and incubated at room temperature for 1 hour (anti-BRCA1 Abcam MS110 diluted 1:200; anti-Geminin (ProteinTech Group, 10802-1-AP, diluted 1:400). Sections were washed for 5 minutes in DAKO Wash Buffer followed by 5 minutes in blocking buffer. Secondary antibodies (Alexa Fluor 488 or 568) were diluted 1:500 in blocking buffer and incubated for 30 minutes at room temperature. The 2-step washing was repeated followed by 5 minutes incubation in distilled water. Dehydration was performed with increasing concentrations of ethanol. Sections were mounted with

DAPI ProLong Gold antifade reagent and stored at -20°C. For analyses tumors from 2 mice per treatment group were analyzed and counted. For each tumor a minimum of 100 geminin-positive cells were identified and counted for those that had at least 5 BRCA1 foci. BRCA1 foci positive cells were calculated as a percentage of geminin-positive cells.

For assessment of Ki-67 and γ-H2AX by IHC, slides were deparaffinized and hydrated. Antigen retrieval was performed using pH 9 EDTA buffer (DAKO, S2368). Endogenous peroxidases were quenched by immersion of slides in 3% hydrogen peroxide solution (30% H2O2, Fisher BP2633-500, diluted in methanol). Primary antibody Ki-67 (Clone EP5), Epitomics, (1:1500) or γ-H2AX [pS139] (N1-4131, EMD) (1,20,000) were diluted with DaVinci Green Diluant (Biocare Medical, PD900) and incubated on slides overnight at 4 degrees in a humidified slide chamber. Slides were then washed 3x in TBST and incubated with Envision+ System HRP Labelled Polymer Anti-Rabbit (Dako, K4003) for 1 hour at room temperature. Specimens were washed 3x in TBST and then developed with DAB solution (DAKO, K3468) and counterstained in Meyer's Hematoxylin (Dako, S3309). For analyses of Ki67 and γ-H2AX expression, a minimum of 2 tumors derived from 2 separate mice we used. Mice were treated with rucaparib 150 mg/kg two times per day for 4 continuous days. For cisplatin, mice were treated with a single dose of 6 mg/kg. Tumors were resected and formalin fixed 4 days from the first dose. A minimum of 2 tumors and 3 images per tumor were used to calculate staining intensities. Image staining intensities were measured using Image J analyses software.

PDX tumor derivation, xenograft treatments and analyses

For patient-derived xenografts, patient consent for tumor use in animals was completed under a protocol approved by the Vall d'Hebron Hospital Clinical Investigation Ethical Committee and Animal Use Committee. Mice were maintained and treated in accordance with institutional guidelines of Vall d'Hebron University Hospital Care and Use Committee. Tumors were subcutaneously implanted in 6 week old female HsdCpb:NMRI-*Foxn1*^{nu} mice (Harlan Laboratories, Italy). Animals were supplemented with 1μM estradiol (Sigma) in the drinking water. Upon xenograft growth, tumor tissue was re-implanted into recipient mice, which were randomized upon implant growth. Mice were allocated in control/treated groups to deliver similar mean and standard error when tumor volume reached between 150-300 mm^3 without any blinding. Vehicle or olaparib was administered at 50mg/kg per oral gavage six days per week. Tumor xenografts were measured with calipers and tumor volumes were determined using the formula: (length x width^2) Å~(π/6). At the end of the experiment, animals were killed by CO2 inhalation. Tumor volumes are plotted as mean ± S.E.M. RTV for vehicle treated mice, and individual relative tumor volumes are shown for olaparib treated mice. For xenograft studies, MDA-MB-436 cells were subcutaneously implanted in 6 week old female NSG mice (NOD.Cg-*Prkdc*^{scid} *Il2rg*^{tm1Wjl}/SzJ). When tumors reached approximately 300 mm^3 tumors were harvested and cut up into smaller pieces followed by subcutaneous re-implantation. Treatment was initiated when tumors reached between 150-180 mm^3. Rucaparib was administered at 150 mg/kg twice daily for 10 continuous days with a 2-day break after the first 5 days. Cisplatin was administered at a single dose of 6 mg/kg. Tumors were measured with calipers and tumor volumes calculated as described above.

Measurements were carried out every 2 days and mice were euthanized when tumors reached 1500 mm^3 in accordance with institutional guidelines of Fox Chase Cancer Center.

Statistical analyses

Mean and standard error values were compared using unpaired *t*-tests (GraphPad Software). $P < 0.05$ was considered statistically significant. *'s indicate statistically significant *P* values. There were similar variances between statistical groups compared. All statistical tests were unpaired *t*-tests unless otherwise stated next to the *P* value.

Results

Cell lines with exon 11 mutations express BRCA1-Δ11q. To examine the impact of *BRCA1* exon 11 mutations on the expression of BRCA1 proteins, we employed a panel of human cancer cell lines that were either *BRCA1* wild-type or harbored known deleterious *BRCA1* mutations (Supplementary Fig. S2A). Full-length BRCA1 protein was detectable in MDA-MB-231, MCF7 and MDA-MB-468 wild-type *BRCA1* cell lines, but was absent in all *BRCA1* mutation containing cell lines. A band corresponding with the predicted molecular weight (~89 kDa) of the BRCA1-Δ11q isoform was present in *BRCA1* wild-type cell lines, as well as L56Br-C1, SUM149PT and UWB1.289 cell lines that harbored *BRCA1* exon 11 frameshift mutations (Fig. 1A).

To establish the identity of the isoform detected below the 100-kDa mark, we transfected cells with an siRNA designed to specifically target BRCA1-Δ11q and measured protein expression. BRCA1-Δ11q siRNA did not impact the levels of the full-length, but dramatically reduced the expression of the predicted BRCA1-Δ11q isoform (Fig. 1B). Furthermore, we confirmed that cells did not harbor secondary *BRCA1* reversion mutations or genomic rearrangements (Supplementary Fig. S2).

Next we investigated the levels of *BRCA1* mRNA containing exon 11 (+11) as well as the *BRCA1-Δ11q* (Δ11q) isoform expression. L56Br-C1, SUM149PT and UWB1.289 exon 11 mutant cell lines exhibited 3- ($P < 0.001$), 3- ($P < 0.001$) and 2.9-fold ($P < 0.001$) lower expression of +11 transcripts, respectively, relative to MDA-MB-231 cells (Fig. 1C). In contrast, relative Δ11q expression was 1.46- ($P = 0.0148$), 1.55- ($P < 0.001$) and 1.58-fold ($P = 0.0136$) higher in L56Br-C1, SUM149PT and UWB1.289, respectively, relative to MDA-MB-231 cells expression levels (Fig. 1C).

Robust BRCA1 gene transcription promotes BRCA1-Δ11q expression. To investigate the impact of germline mutations on exon 11 splicing, we introduced a series of exon 11 frameshift mutations into a BRCA1-minigene system (Supplementary Fig. S3). Mutation of the exon 11q splice junction disrupted Δ11q-reporter mRNA and protein expression. However, three different frameshift mutations at various locations throughout exon 11 had no effect on Δ11q-reporter expression (Fig. 1D). Moreover, RNA-seq analyses of mRNA splice junctions did not indicate that higher levels of *BRCA1-Δ11q* expression in

cell lines with exon 11 mutations were due to increased global alterations in splicing (Supplementary Table S1).

To further investigate the effects of exon 11 mutations on *BRCA1-Δ11q* levels, we used CRISPR/Cas9 technology to generate SUM149PT cells that either had additional out of frame mutations, or reversion mutations that restored the reading frame (Supplementary Fig. S4). In line with minigene data, the introduction of additional out of frame or frame restoring mutations in exon 11 did not affect *BRCA1-Δ11q* expression (Fig. 1E). However, clones 3 and 4 that had restored *BRCA1* reading frames, expressing the BRCA1-long-form protein product, had 2.5- ($P < 0.0001$) and 2.47-fold ($P < 0.0001$) increased levels of +11 expression, respectively, relative to sg_GFP control cells (Fig. 1E); likely resulting from premature translation termination codon (PTC) removal, enabling +11 containing transcripts to avoid NMD (3).

We confirmed that NMD contributed to the low levels of +11 mRNA detected in exon 11 mutation containing cell lines by treating cells with cycloheximide (CHX), an inhibitor of NMD (38) (Fig. 1F). CHX treatment for five hours resulted in a 2.8- ($P = 0.0007$), 3.2- ($P = 0.023$) and 2.9-fold ($P = 0.0024$) increase in +11 levels in L56Br-C1, SUM149PT and UWB1.289 exon 11 mutant cell lines, respectively, but did not affect +11 levels in wild-type MDA-MB-231 cells, or Δ11q mRNA levels in any of the cell lines (Fig. 1F).

The increase in +11 mRNA resulting from inhibition of NMD led us to predict that exon 11 mutant cell lines have robust *BRCA1* gene transcription. To test this possibility, we

treated cells with the transcription inhibitor actinomycin D (ACT) and measured *BRCA1* mRNA levels. MDA-MB-231 cells treated with ACT had a 1.4-fold ($P = 0.0002$) reduction in +11 mRNA levels compared to vehicle treated cells. However, ACT treatment reduced +11 levels 3-fold ($P = 0.0133$) in SUM149PT cells compared to vehicle treated cells, and completely abrogated the CHX-mediated increase in +11 mRNA (Fig. 1G). ACT also reduced Δ11q levels 1.6-fold ($P = 0.002$) and 2-fold ($P = 0.021$) in MDA-MB-231 and SUM149PT cells, respectively, compared to vehicle treatments (Fig. 1H).

Exon 11 mutant cells demonstrate partial PARPi and cisplatin resistance. We next measured the ability of exon 11 mutant cells to form BRCA1 and RAD51 foci. *BRCA1* wild-type as well as exon 11 mutant cell lines formed robust BRCA1 and RAD51 γ-irradiation-induced foci (IRIF). In contrast, BRCA1 and RAD51 IRIF were low or undetectable in cells that harbored *BRCA1* mutations outside of exon 11 (Fig. 2A). SUM1315MO2, HCC1395 and MDA-MB-436 cell lines were highly sensitive to treatment with the PARP inhibitors rucaparib and olaparib. In contrast, exon 11 mutation containing L56Br-C1, SUM149PT and UWB1.289 cells displayed intermediate PARPi sensitivity. SUM1315MO2, HCC1395 and MDA-MB-436 cell lines were also more sensitive to cisplatin treatment compared to L56Br-C1, SUM149PT and UWB1.289 cells. The presence of *BRCA1* exon 11 mutations did not impact taxol sensitivity (Fig. 2B and Supplementary Table S2).

In cell growth experiments, *BRCA1* wild-type cells continuously cultured in the presence of PARPi or cisplatin proliferated at the same rate as vehicle treated cells (Fig. 2C). Exon 11 mutant cell lines proliferated at a reduced rate in the presence of PARPi or cisplatin (Fig. 2C). MDA-MB-436 and HCC1395 cell lines harbor BRCT domain mutations and lost viability in the presence of PARPi or cisplatin. PARPi and cisplatin initially had a greater impact on the proliferation rate of UWB1.289 cells, but over time proliferation gradually increased, and corresponded with increased expression of BRCA1-Δ11q (Fig. 2D). Importantly, depletion of the BRCA1-Δ11q using 2 BRCA1 shRNAs reduced RAD51 IRIF 6.8- (P = 0.0021) and 5.7-fold (P = 0.0027) in SUM149PT, as well as 6- (P = 0.0014) and 4.7-fold (P = 0.0016) in UWB1.289 cells, compared to non-target (NT) shRNA cells (Fig. 2E). Furthermore, BRCA1 shRNA sensitized SUM149PT and UWB1.289 cells to both PARPi and cisplatin treatments (Fig. 2F and Supplementary Table S2).

BRCA1-Δ11q is functional but inferior to BRCA1-full-length. To more finely assess the ability of BRCA1-Δ11q to provide resistance to therapy, we used CRISPR/Cas9-mediated gene editing to modify *BRCA1* in SUM149PT cells (Supplementary Fig. S4). SUM149PT cells were subject to an sg_GFP control, or sg_exon11 targeting the mutation-containing region of exon 11. Mutations introduced by sg_exon11 were either out of frame (out-frame) or restored the *BRCA1* reading frame (in-frame). Moreover, cell lines that expressed sg_exon22 demonstrated frameshift mutations in exons 22, resulting in loss of BRCA1-Δ11q expression (Fig. 3A and Supplementary Fig. S4). BRCA1-Δ11q expression in sg_exon11 treated clones with unrestored reading frames was identical to

sg_GFP control cells and there were no differences in PARPi and cisplatin sensitivity in colony formation assays. However, sg_exon11 in-frame clone 3 was 226- ($P = 0.0174$) and 3.7-fold ($P = 0.0009$) more resistant to PARPi and cisplatin, respectively, and clone 4 was 207- ($P < 0.0001$) and 3.6-fold ($P = 0.0058$) more resistant to PARPi and cisplatin, respectively, compared to sg_GFP cells. In contrast, sg_exon22 cells were 31.4- ($P = 0.0183$) and 2.3-fold ($P = 0.0059$) more sensitive to PARPi and cisplatin, respectively, compared to sg_GFP cells (Fig. 3B).

We also compared the ability of ectopic BRCA1 full-length and BRCA1-Δ11q to rescue PARPi and cisplatin sensitivity (Fig. 3C). MDA-MB-436 cells harbor a *BRCA1*$^{5396+1G>A}$ mutation that results in protein misfolding, undetectable BRCA1 protein and RAD51 IRIF, as well as exquisite PARPi and cisplatin sensitivity (20, 39, 40). MDA-MB-436 cells expressing BRCA1-full-length demonstrated robust rescue and were 179- ($P = 0.0063$) and 4.6-fold ($P = 0.0002$) more resistant to PARPi and cisplatin, respectively, compared to mCherry control cells. BRCA1-Δ11q was less effective at rescue, and cells were 19- ($P = 0.0493$) and 2.8-fold ($P = 0.0004$) more resistant to PARPi and cisplatin, respectively, compared to mCherry control cells (Fig. 3D). Moreover, when we introduced an L304P mutation (equivalent to L1407P in full-length BRCA1) that blocks the BRCA1-PALB2 interaction (41), BRCA1-Δ11q mediated-PARPi and cisplatin rescue was abolished (Fig. 3D).

Both BRCA1-full-length and BRCA1-Δ11q expressing cells formed BRCA1 and RAD51 IRIF. However, BRCA1-Δ11q expressing cells exhibited 1.9- ($P = 0.0053$) and 1.9-fold

(P = 0.0141) lower levels of BRCA1 and RAD51 IRIF, respectively, than full-length BRCA1 expressing cells, while BRCA1-Δ11q+ L304P expressing cells had undetectable BRCA1 and RAD51 IRIF (Fig. 3E). Immunoprecipitation of ectopic BRCA1 from MDA-MB-436 cells suggested that BRCA1-Δ11q interacted, although less efficiently, with functional protein partners for full-length BRCA1 (Fig. 3F). We also demonstrated ectopic BRCA1-Δ11q provided therapy resistance in HCC1395 cells and in a mouse embryonic stem cell system (42) (Supplementary Fig. S5).

BRCA1-Δ11q promotes resistance in vivo. To examine the significance of *BRCA1-Δ11q* expression in tumors, we first measured PARPi responsiveness and *BRCA1* isoform expression in two individual *BRCA1* exon 11 mutant patient-derived xenograft (PDX) models. Despite both PDX models harboring the same *BRCA1*-exon 11 2080delA mutation (Supplementary Fig. S2), PDX124 tumors were sensitive and PDX196 tumors were resistant to olaparib treatment (Fig. 4A). We confirmed that tumors did not have reversion mutations or gene rearrangements (Supplementary Fig. S2). Similar to exon 11 mutant cell lines, both PDX124 and PDX196 expressed higher levels of Δ11q compared to +11 mRNA, relative to MDA-MB-231 control cells. However, *BRCA1* mRNA levels were significantly greater in PDX196 tumors than in PDX124 tumors, with 26- (P = 0.0001) and 23-fold (P < 0.0001) higher levels of both +11 and Δ11q, respectively (Fig. 4B). BRCA1-Δ11q protein expression was detectable in olaparib resistant PDX196 tumors, as well as PDX124 tumors that eventually grew through olaparib treatment (Fig. 4C). BRCA1 foci formation was also readily detectable in PDX196 tumors (Fig. 4D).

To further assess the impact of BRCA1-Δ11q on therapy resistance *in vivo*, we utilized the MDA-MB-436 isogenic cell line panel for xenograft experiments. At 30 days post tumor implantation, rucaparib or cisplatin treatment delayed mean tumor growth 6.8- ($P < 0.0001$) and 12.9-fold ($P < 0.0001$), respectively, compared to vehicle treated mice with mCherry overexpressing MDA-MB-436 tumors. In contrast, rucaparib and cisplatin treatment delayed mean tumor growth 1.1-fold ($P = 0.4455$) and 1.28-fold ($P = 0.2537$) in BRCA1-wild-type and 1.4-fold ($P = 0.0872$) and 2.3-fold ($P = 0.019$) in BRCA1-Δ11q overexpressing tumors, respectively, compared to vehicle treated mice (Fig. 4 E,F).

Kaplan-Meier analyses indicated that the median overall survival (OS) of mice harboring mCherry expressing tumors that were treated with rucaparib or cisplatin increased 1.7-fold ($P = 0.0016$, log-rank test) and 2-fold ($P = 0.0016$, log-rank test), respectively, compared to vehicle treated mice. In contrast, in mice harboring BRCA1 wild-type tumors that were treated with rucaparib or cisplatin, median OS increased 1.3-fold ($P = 0.0071$, log-rank test) and 1.4-fold ($P = 0.0048$, log-rank test), respectively, and in mice harboring BRCA1-Δ11q tumors treated with rucaparib or cisplatin median OS increased 1.2-fold ($P = 0.1536$, log-rank test) and 1.5-fold ($P = 0.0333$, log-rank test), respectively, compared to vehicle treated mice (Fig. 4G).

Short-term assessment of pharmacodynamics markers showed that rucaparib increased γ-H2AX positivity similarly in all tumors, but wild-type and BRCA1-Δ11q tumors had 4.5-($P < 0.0001$) and 2.2-fold ($P = 0.005$) lower γ-H2AX positivity, respectively, after cisplatin treatment compared to mCherry expressing tumors. Additionally, wild-type and

BRCA1-Δ11q tumors treated with rucaparib had 2.2- (P = 0.0007) and 2.5-fold (P = 0.0059) higher Ki67 positivity, respectively; and tumors treated with cisplatin had 2.6- (P < 0.0001) and 3.7-fold (P = 0.0003) higher Ki67 positivity, respectively, compared to mCherry expressing tumors (Fig. 4G). In contrast to *in vitro* data, the degree of PARPi or cisplatin rescue afforded by BRCA1-Δ11q overexpression was more similar to BRCA1 full-length *in vivo.*

Assessment of BRCA1 exon 11 mutations and patient survival. Because exon 11 mutant tumors were capable of expressing *BRCA1-Δ11q*, we assessed survival outcomes of patients with frameshift mutations located inside (IE11) versus outside (OE11) of exon 11. We analyzed 5-year overall survival data from the time of initial diagnosis in patients with serous ovarian carcinoma from a previously reported study (43). Here, participants with *BRCA1* frameshift mutations OE11 (n = 231, 43%; 95% CI, 36%-49%) presented better OS than noncarriers (n = 1333, 33%; 95% CI, 30%-36%) (P = 0.002, Log rank test) as well as participants with frameshift mutations IE11 (n = 148, 31%; 95% CI, 23%-39%) (P = 0.02, Log rank test) at 5 years of follow up. Moreover, participants with frameshift mutations IE11 presented with 5-year OS similar to noncarriers (P = 0.84, Log rank test) (Fig. 5A, Supplementary Tables S3 and S4).

Although patients with exon 11 mutations demonstrated worse 5-year survival, we hypothesized that, similar to our PDX data, *BRCA1-Δ11q* might only be highly expressed in a fraction of exon 11 mutant tumors, and so not all exon 11 mutant patients would necessarily be resistant to therapy. Analyses of primary tumors (unrelated to the above

studies) with mutations IE11 showed variable levels of *BRCA1-Δ11q* expression. Tumor #317 expressed 2.7- ($P = 0.0227$) and 4-fold ($P = 0.0117$) greater levels of Δ11q compared to tumor #325 and tumor #411, respectively, despite all tumors harboring deleterious exon 11 mutations (Fig. 5A).

Inhibition of splicing increases PARPi sensitivity. Because high levels of BRCA1-Δ11q expression were required for residual function, we hypothesized that limiting splicing-dependent excision of exon 11q might provide an opportunity to enhance PARPi sensitivity. We first identified two binding elements for the FOX2 splicing site selection factor at position +18 and +63 downstream from the cryptic splice site location (Supplementary Fig. S6) (44, 45). Depletion of FOX2 using 2 individual siRNAs did not impact +11 expression levels, but reduced Δ11q expression 1.7- ($P = 0.0043$) and 1.6-fold ($P = 0.0179$) in MDA-MB-231, 1.5- ($P = 0.048$) and 1.6-fold ($P = 0.0301$) in UWB1.289, 2.2- ($P = 0.0056$) and 3.1-fold ($P = 0.0017$) in SUM149PT cells, compared to scrambled siRNA treated cells, respectively (Fig. 6A). At the protein level, densitometric analyses of Western blots indicated FOX2 siRNA did not impact full-length BRCA1 protein expression, but BRCA1-Δ11q levels were reduced 2.9- and 2.2-fold in MDA-MB-231, 2- and 2.8-fold in UWB1.289, 1.9- and 1.8-fold in SUM149PT cells, compared to scrambled siRNA treated cells (Fig. 6B). FOX2 siRNA had no impact on MDA-MB-231 cells PARPi sensitivity, but reduced the LC50 value of rucaparib 3.8-($P = 0.0063$) and 27.4-fold ($P = 0.0017$) in UWB1.289 cells, as well as 1.9- ($P = 0.0237$) and 5-fold ($P = 0.0002$) in SUM149PT cells, compared to scrambled siRNA treated cells

(Fig. 6C). Furthermore, BRCA1-minigene analyses demonstrated that mutation of FOX2 binding motifs also partially decreased Δ11q-reporter mRNA and protein levels (Fig. 6D).

We next investigated the ability of pladienolide B (Pl-B), a small molecule inhibitor of the U2 snRNP spliceosome machinery(46), to disrupt *BRCA1-Δ11q* production. Pl-B treatment reduced both +11 and Δ11q mRNA expression, however the relative reduction in Δ11q levels was 7.7- ($P = 0.002$) and 7-fold ($P = 0.016$) greater compared to the reduction in +11 levels in MDA-MB-231 and UWB1.289 cells, respectively (Fig. 6E). Furthermore, full-length BRCA1 protein levels were reduced but remained readily detectable after treatment with up to 10 nM Pl-B in MDA-MB-231 cells. However, BRCA1-Δ11q protein levels were barely detectable at 1.25 nM Pl-B in both MDA-MB-231 and UWB1.289 cells (Fig. 6F). Simultaneous incubation with both Pl-B and rucaparib did not significantly impact MDA-MB-231 cells, but resulted in a 2.8- ($P = 0.0296$) and 2.1-fold ($P = 0.0426$) reduction in colony formation compared to cells treated with rucaparib only in UWB1.289 and SUM149PT cells, respectively (Fig. 6G). Furthermore, ectopic overexpression of a BRCA1-Δ11q cDNA that did not depend on exon 11q splicing, resulted in a 1.9-fold ($P = 0.001$) rescue in colony formation in cells treated with the Pl-B and rucaparib combination, compared to GFP expressing control cells (Fig. 6H); suggesting that Pl-B-induced PARPi sensitization was mediated, in part, through the reduction in BRCA1-Δ11q levels.

Discussion

In the current study, we provide evidence that *BRCA1* splice isoforms lacking exon 11 are capable of producing truncated but hypomorphic proteins. It was previously shown that the exon 11 deficient Brca1-Δ11 isoform partially compensates for the lack of other Brca1 isoforms during embryogenesis (31-33, 47). Here, we show that BRCA1-Δ11q can also partially compensate for full-length BRCA1 in response to homologous recombination targeting therapeutics. BRCA1-Δ11q retains, although less efficiently, many of the protein-protein interactions carried out by full-length BRCA1. We identified the BRCA1-Δ11q-PALB2 interaction as critical for BRCA1-Δ11q-mediated RAD51 IRIF and resistance.

BRCA1-Δ11q was expressed in *BRCA1* wild-type as well as exon 11 mutant cell lines. Although frameshift mutations in exon 11 resulted in the NMD of exon 11 containing-transcripts, they did not impact the rate of alternative splicing or directly affect *BRCA1-Δ11q* levels. In support of this, PDX124 and PDX196 tumors both harbored identical 2080delA exon 11 mutations; however, both +11 and Δ11q transcript levels were significantly higher in PDX196 relative to PDX124 tumors, suggesting that overall *BRCA1* gene transcription, rather than the rate of alternative exon splicing, was elevated. Both patients whose tumors were used to derive PDX124 and PDX196 initially demonstrated clinical responsiveness to olaparib therapy; while PDX124 was derived prior to the patient starting olaparib therapy, PDX196 was derived at the time of clinical tumor progression on olaparib. We anticipate that high levels of *BRCA1-Δ11q* expression may be selected for in response to chemotherapy. Primary patient tumors harboring exon

11 mutations also demonstrated variable *BRCA1-Δ11q* levels, and this isoform might only be overexpressed in a subset of exon 11 mutation carriers. Additional resistance mechanisms such as secondary reversion mutations have also been shown to occur in tumors with exon 11 mutations (48, 49).

Intriguingly, our analyses indicated that exon 11 mutation carriers with ovarian cancer had a worse 5-year overall survival compared to non-exon 11 mutation carriers (Fig. 5A). Another recent study of mutation-specific cancer risks identified the exon 11 region of *BRCA1* as an ovarian cancer cluster region, where mutation carriers had a relative decrease in breast relative to ovarian cancer risk (50). Further work is required to determine if BRCA1-Δ11q has any impact on long-term survival outcomes or breast versus ovarian tissue specific phenotypes.

Currently, an understanding of PARPi and platinum resistance is incomplete. Our findings provide evidence for a role of the BRCA1-Δ11q alternative splice isoform in promoting resistance. Moreover, we show that inhibition of the spliceosome reduced BRCA1-Δ11q levels and sensitized exon 11 mutant cell lines to PARPi, potentially offering a strategy to re-sensitize tumors that express high levels of BRCA1-Δ11q.

Acknowledgments

This work was supported by US National Institutes of Health (NIH) Grants P50 CA083638 [Fox Chase Cancer Center (FCCC) Specialized Program of Research Excellence (SPORE) in Ovarian Cancer and R21CA191690, 5P30 CA006927 (FCCC Developmental New Investigator funds), Susan G. Komen Career Catalyst Award CCR12226280, and OC130212 Department of Defense Ovarian Academy Award, Basser Center for BRCA pilot project award (N.J.), P50 CA83636 (Pacific Ovarian Cancer Research Consortium SPORE in Ovarian Cancer), the Wendy Feuer Ovarian Cancer Research Fund (E.M.S.). M.H.G. was supported by the Intramural Research Program of the US National Cancer Institute. Rucaparib was supplied by Clovis Oncology. We thank the FCCC Biostatistics and bioinformatics, Biorepository and Genomics facilities. J.B. is recipient of an Instituto de Salut Carlos III (ISCIII) grant PI12/02606. This work was also supported by a GHD/FERO grant (V.S.). The authors thank Yasir H. Ibrahim, Pilar Antón, Ana Vivancos, Orland Diaz, Michael Slifker, Yusheng Li for helpful experimental support and data analysis.

References

1. Szabo, C.I., and King, M.C. 1995. Inherited breast and ovarian cancer. *Hum Mol Genet* 4 Spec No:1811-1817.
2. Friedman, L.S., Ostermeyer, E.A., Szabo, C.I., Dowd, P., Lynch, E.D., Rowell, S.E., and King, M.C. 1994. Confirmation of BRCA1 by analysis of germline mutations linked to breast and ovarian cancer in ten families. *Nat Genet* 8:399-404.
3. Perrin-Vidoz, L., Sinilnikova, O.M., Stoppa-Lyonnet, D., Lenoir, G.M., and Mazoyer, S. 2002. The nonsense-mediated mRNA decay pathway triggers degradation of most BRCA1 mRNAs bearing premature termination codons. *Hum Mol Genet* 11:2805-2814.
4. Moynahan, M.E., Cui, T.Y., and Jasin, M. 2001. Homology-directed dna repair, mitomycin-c resistance, and chromosome stability is restored with correction of a Brca1 mutation. *Cancer Res* 61:4842-4850.
5. Scully, R., Chen, J., Ochs, R.L., Keegan, K., Hoekstra, M., Feunteun, J., and Livingston, D.M. 1997. Dynamic changes of BRCA1 subnuclear location and phosphorylation state are initiated by DNA damage. *Cell* 90:425-435.
6. Lord, C.J., Tutt, A.N., and Ashworth, A. 2015. Synthetic lethality and cancer therapy: lessons learned from the development of PARP inhibitors. *Annu Rev Med* 66:455-470.
7. Lord, C.J., and Ashworth, A. 2013. Mechanisms of resistance to therapies targeting BRCA-mutant cancers. *Nat Med* 19:1381-1388.

8. Bryant, H.E., Schultz, N., Thomas, H.D., Parker, K.M., Flower, D., Lopez, E., Kyle, S., Meuth, M., Curtin, N.J., and Helleday, T. 2005. Specific killing of BRCA2-deficient tumours with inhibitors of poly(ADP-ribose) polymerase. *Nature* 434:913-917.

9. Farmer, H., McCabe, N., Lord, C.J., Tutt, A.N., Johnson, D.A., Richardson, T.B., Santarosa, M., Dillon, K.J., Hickson, I., Knights, C., et al. 2005. Targeting the DNA repair defect in BRCA mutant cells as a therapeutic strategy. *Nature* 434:917-921.

10. Kennedy, R.D., Quinn, J.E., Mullan, P.B., Johnston, P.G., and Harkin, D.P. 2004. The role of BRCA1 in the cellular response to chemotherapy. *J Natl Cancer Inst* 96:1659-1668.

11. Quinn, J.E., Kennedy, R.D., Mullan, P.B., Gilmore, P.M., Carty, M., Johnston, P.G., and Harkin, D.P. 2003. BRCA1 functions as a differential modulator of chemotherapy-induced apoptosis. *Cancer Res* 63:6221-6228.

12. Gelmon, K.A., Tischkowitz, M., Mackay, H., Swenerton, K., Robidoux, A., Tonkin, K., Hirte, H., Huntsman, D., Clemons, M., Gilks, B., et al. 2011. Olaparib in patients with recurrent high-grade serous or poorly differentiated ovarian carcinoma or triple-negative breast cancer: a phase 2, multicentre, open-label, non-randomised study. *Lancet Oncol* 12:852-861.

13. Sandhu, S.K., Schelman, W.R., Wilding, G., Moreno, V., Baird, R.D., Miranda, S., Hylands, L., Riisnaes, R., Forster, M., Omlin, A., et al. 2013. The poly(ADP-ribose) polymerase inhibitor niraparib (MK4827) in BRCA mutation carriers and

patients with sporadic cancer: a phase 1 dose-escalation trial. *Lancet Oncol* 14:882-892.

14. Ang, J.E., Gourley, C., Powell, B., High, H., Shapira-Frommer, R., Castonguay, V., De Greve, J., Atkinson, T., Yap, T.A., Sandhu, S., et al. 2013. Efficacy of chemotherapy in BRCA1/2 mutation carrier ovarian cancer in the setting of poly(ADP-ribose) polymerase inhibitor resistance: a multi-institutional study. *Clin Cancer Res*.

15. Ledermann, J., Harter, P., Gourley, C., Friedlander, M., Vergote, I., Rustin, G., Scott, C.L., Meier, W., Shapira-Frommer, R., Safra, T., et al. 2014. Olaparib maintenance therapy in patients with platinum-sensitive relapsed serous ovarian cancer: a preplanned retrospective analysis of outcomes by BRCA status in a randomised phase 2 trial. *Lancet Oncol* 15:852-861.

16. Edwards, S.L., Brough, R., Lord, C.J., Natrajan, R., Vatcheva, R., Levine, D.A., Boyd, J., Reis-Filho, J.S., and Ashworth, A. 2008. Resistance to therapy caused by intragenic deletion in BRCA2. *Nature* 451:1111-1115.

17. Sakai, W., Swisher, E.M., Karlan, B.Y., Agarwal, M.K., Higgins, J., Friedman, C., Villegas, E., Jacquemont, C., Farrugia, D.J., Couch, F.J., et al. 2008. Secondary mutations as a mechanism of cisplatin resistance in BRCA2-mutated cancers. *Nature* 451:1116-1120.

18. Bouwman, P., Aly, A., Escandell, J.M., Pieterse, M., Bartkova, J., van der Gulden, H., Hiddingh, S., Thanasoula, M., Kulkarni, A., Yang, Q., et al. 2010. 53BP1 loss rescues BRCA1 deficiency and is associated with triple-negative and BRCA-mutated breast cancers. *Nat Struct Mol Biol* 17:688-695.

19. Bunting, S.F., Callen, E., Wong, N., Chen, H.T., Polato, F., Gunn, A., Bothmer, A., Feldhahn, N., Fernandez-Capetillo, O., Cao, L., et al. 2010. 53BP1 inhibits homologous recombination in Brca1-deficient cells by blocking resection of DNA breaks. *Cell* 141:243-254.

20. Johnson, N., Johnson, S.F., Yao, W., Li, Y.C., Choi, Y.E., Bernhardy, A.J., Wang, Y., Capelletti, M., Sarosiek, K.A., Moreau, L.A., et al. 2013. Stabilization of mutant BRCA1 protein confers PARP inhibitor and platinum resistance. *Proc Natl Acad Sci U S A* 110:17041-17046.

21. Drost, R., Bouwman, P., Rottenberg, S., Boon, U., Schut, E., Klarenbeek, S., Klijn, C., van der Heijden, I., van der Gulden, H., Wientjens, E., et al. 2011. BRCA1 RING function is essential for tumor suppression but dispensable for therapy resistance. *Cancer Cell* 20:797-809.

22. Rottenberg, S., Jaspers, J.E., Kersbergen, A., van der Burg, E., Nygren, A.O., Zander, S.A., Derksen, P.W., de Bruin, M., Zevenhoven, J., Lau, A., et al. 2008. High sensitivity of BRCA1-deficient mammary tumors to the PARP inhibitor AZD2281 alone and in combination with platinum drugs. *Proc Natl Acad Sci U S A* 105:17079-17084.

23. Colombo, M., Blok, M.J., Whiley, P., Santamarina, M., Gutierrez-Enriquez, S., Romero, A., Garre, P., Becker, A., Smith, L.D., De Vecchi, G., et al. 2014. Comprehensive annotation of splice junctions supports pervasive alternative splicing at the BRCA1 locus: a report from the ENIGMA consortium. *Hum Mol Genet* 23:3666-3680.

24. Thomassen, M., Blanco, A., Montagna, M., Hansen, T.V., Pedersen, I.S., Gutierrez-Enriquez, S., Menendez, M., Fachal, L., Santamarina, M., Steffensen, A.Y., et al. 2012. Characterization of BRCA1 and BRCA2 splicing variants: a collaborative report by ENIGMA consortium members. *Breast Cancer Res Treat* 132:1009-1023.

25. Romero, A., Garcia-Garcia, F., Lopez-Perolio, I., Ruiz de Garibay, G., Garcia-Saenz, J.A., Garre, P., Ayllon, P., Benito, E., Dopazo, J., Diaz-Rubio, E., et al. 2015. BRCA1 Alternative splicing landscape in breast tissue samples. *BMC Cancer* 15:219.

26. Orban, T.I., and Olah, E. 2001. Expression profiles of BRCA1 splice variants in asynchronous and in G1/S synchronized tumor cell lines. *Biochem Biophys Res Commun* 280:32-38.

27. Tammaro, C., Raponi, M., Wilson, D.I., and Baralle, D. 2012. BRCA1 exon 11 alternative splicing, multiple functions and the association with cancer. *Biochem Soc Trans* 40:768-772.

28. Raponi, M., Smith, L.D., Silipo, M., Stuani, C., Buratti, E., and Baralle, D. 2014. BRCA1 exon 11 a model of long exon splicing regulation. *RNA Biol* 11:351-359.

29. Orban, T.I., and Olah, E. 2003. Emerging roles of BRCA1 alternative splicing. *Mol Pathol* 56:191-197.

30. Wilson, C.A., Payton, M.N., Elliott, G.S., Buaas, F.W., Cajulis, E.E., Grosshans, D., Ramos, L., Reese, D.M., Slamon, D.J., and Calzone, F.J. 1997. Differential subcellular localization, expression and biological toxicity of BRCA1 and the splice variant BRCA1-delta11b. *Oncogene* 14:1-16.

31. Ludwig, T., Chapman, D.L., Papaioannou, V.E., and Efstratiadis, A. 1997. Targeted mutations of breast cancer susceptibility gene homologs in mice: lethal phenotypes of Brca1, Brca2, Brca1/Brca2, Brca1/p53, and Brca2/p53 nullizygous embryos. *Genes Dev* 11:1226-1241.

32. Xu, X., Qiao, W., Linke, S.P., Cao, L., Li, W.M., Furth, P.A., Harris, C.C., and Deng, C.X. 2001. Genetic interactions between tumor suppressors Brca1 and p53 in apoptosis, cell cycle and tumorigenesis. *Nat Genet* 28:266-271.

33. Xu, X., Wagner, K.U., Larson, D., Weaver, Z., Li, C., Ried, T., Hennighausen, L., Wynshaw-Boris, A., and Deng, C.X. 1999. Conditional mutation of Brca1 in mammary epithelial cells results in blunted ductal morphogenesis and tumour formation. *Nat Genet* 22:37-43.

34. Breast Cancer Information Core (https://research.nhgri.nih.gov/projects/bic/index.shtml).

35. Thompson, D., Easton, D., and Breast Cancer Linkage, C. 2002. Variation in BRCA1 cancer risks by mutation position. *Cancer Epidemiol Biomarkers Prev* 11:329-336.

36. Risch, H.A., McLaughlin, J.R., Cole, D.E., Rosen, B., Bradley, L., Fan, I., Tang, J., Li, S., Zhang, S., Shaw, P.A., et al. 2006. Population BRCA1 and BRCA2 mutation frequencies and cancer penetrances: a kin-cohort study in Ontario, Canada. *J Natl Cancer Inst* 98:1694-1706.

37. Risch, H.A., McLaughlin, J.R., Cole, D.E., Rosen, B., Bradley, L., Kwan, E., Jack, E., Vesprini, D.J., Kuperstein, G., Abrahamson, J.L., et al. 2001. Prevalence

and penetrance of germline BRCA1 and BRCA2 mutations in a population series of 649 women with ovarian cancer. *Am J Hum Genet* 68:700-710.

38. Barbier, J., Dutertre, M., Bittencourt, D., Sanchez, G., Gratadou, L., de la Grange, P., and Auboeuf, D. 2007. Regulation of H-ras splice variant expression by cross talk between the p53 and nonsense-mediated mRNA decay pathways. *Mol Cell Biol* 27:7315-7333.

39. Williams, R.S., Chasman, D.I., Hau, D.D., Hui, B., Lau, A.Y., and Glover, J.N. 2003. Detection of protein folding defects caused by BRCA1-BRCT truncation and missense mutations. *J Biol Chem* 278:53007-53016.

40. Williams, R.S., and Glover, J.N. 2003. Structural consequences of a cancer-causing BRCA1-BRCT missense mutation. *J Biol Chem* 278:2630-2635.

41. Sy, S.M., Huen, M.S., and Chen, J. 2009. PALB2 is an integral component of the BRCA complex required for homologous recombination repair. *Proc Natl Acad Sci U S A* 106:7155-7160.

42. Bouwman, P., van der Gulden, H., van der Heijden, I., Drost, R., Klijn, C.N., Prasetyanti, P., Pieterse, M., Wientjens, E., Seibler, J., Hogervorst, F.B., et al. 2013. A high-throughput functional complementation assay for classification of BRCA1 missense variants. *Cancer Discov* 3:1142-1155.

43. Bolton, K.L., Chenevix-Trench, G., Goh, C., Sadetzki, S., Ramus, S.J., Karlan, B.Y., Lambrechts, D., Despierre, E., Barrowdale, D., McGuffog, L., et al. 2012. Association between BRCA1 and BRCA2 mutations and survival in women with invasive epithelial ovarian cancer. *JAMA* 307:382-390.

44. Venables, J.P., Klinck, R., Koh, C., Gervais-Bird, J., Bramard, A., Inkel, L., Durand, M., Couture, S., Froehlich, U., Lapointe, E., et al. 2009. Cancer-associated regulation of alternative splicing. *Nat Struct Mol Biol* 16:670-676.

45. Huang, S.C., Ou, A.C., Park, J., Yu, F., Yu, B., Lee, A., Yang, G., Zhou, A., and Benz, E.J., Jr. 2012. RBFOX2 promotes protein 4.1R exon 16 selection via U1 snRNP recruitment. *Mol Cell Biol* 32:513-526.

46. Kotake, Y., Sagane, K., Owa, T., Mimori-Kiyosue, Y., Shimizu, H., Uesugi, M., Ishihama, Y., Iwata, M., and Mizui, Y. 2007. Splicing factor SF3b as a target of the antitumor natural product pladienolide. *Nat Chem Biol* 3:570-575.

47. Huber, L.J., Yang, T.W., Sarkisian, C.J., Master, S.R., Deng, C.X., and Chodosh, L.A. 2001. Impaired DNA damage response in cells expressing an exon 11-deleted murine Brca1 variant that localizes to nuclear foci. *Mol Cell Biol* 21:4005-4015.

48. Norquist, B., Wurz, K.A., Pennil, C.C., Garcia, R., Gross, J., Sakai, W., Karlan, B.Y., Taniguchi, T., and Swisher, E.M. 2011. Secondary somatic mutations restoring BRCA1/2 predict chemotherapy resistance in hereditary ovarian carcinomas. *J Clin Oncol* 29:3008-3015.

49. Patch, A.M., Christie, E.L., Etemadmoghadam, D., Garsed, D.W., George, J., Fereday, S., Nones, K., Cowin, P., Alsop, K., Bailey, P.J., et al. 2015. Whole-genome characterization of chemoresistant ovarian cancer. *Nature* 521:489-494.

50. Rebbeck, T.R., Mitra, N., Wan, F., Sinilnikova, O.M., Healey, S., McGuffog, L., Mazoyer, S., Chenevix-Trench, G., Easton, D.F., Antoniou, A.C., et al. 2015.

Association of type and location of BRCA1 and BRCA2 mutations with risk of breast and ovarian cancer. *JAMA* 313:1347-1361.

Figure legends

Figure 1. *BRCA1* exon 11 mutant cell lines express BRCA1-Δ11q.

(**A**) Cell lines were analyzed for BRCA1 and tubulin levels by Western blot. *Predicted BRCA1 locations, molecular weights are indicated.

(**B**) Cells were treated with scrambled (Sc) or BRCA1-Δ11q (11q) siRNA and analyzed by Western blot.

(**C**) Exon 11 containing (+11) *BRCA1* transcripts and the *BRCA1-Δ11q* (Δ11q) isoform were detected using qRT-PCR. Values were normalized to a HKG, expressed as a percentage of MDA-MB-231 cells.

(**D**) 293T cells were transfected with either GFP-control or BRCA1-minigene reporter constructs that were WT or carrying mutations that disrupted the cryptic 11q splice site (11q), or with frameshift mutations (M1:2288delT; M2:2529C>T; M3:3960C>T). BRCA1-Δ11q-reporter mRNA and protein expression was measured by RT-PCR (*above*) and Western blot (*below*), see Supplementary Fig. S3.

(**E**) CRISPR/Cas9 targeting the mutation-containing region of exon 11 (sg_exon11) generated SUM149PT clones (C) 1-4, see Supplementary Fig. S4. +11 and Δ11q mRNA was measured using qRT-PCR (*left*), values were normalized to a HKG and expressed as a percentage of sg_GFP control cells. BRCA1 protein was detected by Western blot (*right*).

(**F**) The indicated cell lines were treated with vehicle or 10 μg/ml CHX for 5 hours followed by assessment of +11 (*left*) and Δ11q (*right*) levels by qRT-PCR.

(**G**) Cells were treated with either vehicle (V), 10 μg/ml CHX (C), 5 μg/ml ACT (A) or A and C simultaneously for 5 hours and assessed for +11 expression by qRT-PCR.

(**H**) Cells were treated with either vehicle (V), or 5 μg/ml ACT (A) for 5-hours and assessed for Δ11q expression by qRT-PCR. **P* < 0.05.

Figure 2. Exon 11 mutant cells are less sensitive to PARPi and cisplatin treatment.

(**A**) Cells were untreated (no Rx) or treated with IR (10 Gy) and subject to immunofluorescence to detect BRCA1, RAD51 and γ-H2AX foci, representative images of IR treated cells. Mean ± S.E.M foci-positive cells are expressed as a percentage of total geminin positive cells.

(**B**) Cell lines were treated with rucaparib, olaparib, cisplatin or taxol and colony formation assessed; graphs represent three independent experiments, mean ± S.E.M LC50 values; see Supplementary Table S2 for fold changes and *P* values.

(**C**) Cells were maintained in the presence of vehicle, 100 nM rucaparib (*left*) or 20 ng/ml cisplatin (*right*) and counted every 4 days. Cell line growth was expressed as a percentage of vehicle treated cell numbers counted on the same day. Mean ± S.E.M from three technical replicates.

(**D**) UWB1.289 vehicle, rucaparib (R) and cisplatin (C) treated cell lysates were collected at days 25 and 50 for Western blot analysis.

(**E**) Assessment of BRCA1, RAD51 and γ-H2AX foci by immunofluorescence as for (A). Western blot (*above*) shows BRCA1-Δ11q was depleted using 2 individual BRCA1

targeting shRNAs. Representative images (*below*) of IR treated cells and Mean ± S.E.M foci-positive cells are expressed as a percentage of total geminin positive cells (*right*).

(**F**) Cells described in (E) were treated with rucaparib or cisplatin and colony formation assessed; three independent experiments, mean ± S.E.M LC50 concentrations are shown, see Supplementary Table S2. **P* < 0.05.

Figure 3. BRCA1-Δ11q provides partial resistance to therapy *in vitro*.

(**A**) CRISPR/Cas9 gene targeting the SUM149PT *BRCA1* mutation-containing region of exon 11 (sg_exon11) did not affect the reading frame (OF) in clones 1, 2, or restored the reading frame (IF) in clones 3, 4. Targeting of exon 22 (sg_exon22) resulted in frameshift mutations and loss of BRCA1 expression. Cells treated with sg_GFP were used as a control. BRCA1 protein was detected by Western blot. See Supplementary Fig. S4 for more details.

(**B**) Cells described in (A) were treated with rucaparib or cisplatin and colony formation assessed.

(**C**) MDA-MB-436 cells expressing mCherry, BRCA1-full-length, BRCA1-Δ11q or BRCA1-Δ11q+L304P were assessed for BRCA1 protein expression by Western blot.

(**D**) Cells described in (C) were treated with rucaparib or cisplatin and colony formation assessed.

(**E**) Cells described in (C) were treated with IR (10 Gy) and subject to immunofluorescence to detect BRCA1, RAD51 and γ-H2AX foci, as well as geminin and DAPI staining, representative images of IR treated cells. Double geminin and BRCA1 or RAD51 positive cells were counted and expressed as a percentage of total geminin

positive cells, bars show mean ± S.E.M. geminin+BRCA1 or RAD51 foci-positive cells from three independent experiments.

(**F**) Cells described in (C) were subject to immunoprecipitation using an anti-HA antibody and Western blotting with the indicated antibodies. *$P < 0.05$.

Figure 4. BRCA1-Δ11q promotes resistance *in vivo*.

(**A**) PDX124 (n ≥ 8 mice) (*left*) and PDX196 (n ≥ 3 mice) (*right*) tumors were treated with vehicle (black lines) or olaparib (green lines) and tumor volume measured.

(**B**) PDX tumors were harvested from three individual untreated mice and assessed for +11 and Δ11q expression by qRT-PCR. Values were normalized to the *POL2RF* HKG control and expressed as a percentage of the values calculated for MDA-MB-231 cells.

(**C**) MDA-MB-231 cells were prepared for whole cell extract (WCE) as well as tumor xenografts and used as positive controls, and compared to PDX127 (*BRCA1*^{185delAG} mutant control, $n = 1$), PDX196 ($n = 2$), PDX124 OS (growth inhibition with olaparib, $n = 1$) and OR (growth slowed with olaparib, $n = 2$) tumors for Western blotting.

(**D**) Mice harboring PDX196 tumors were treated with vehicle or olaparib and tumors assessed for BRCA1 foci formation as well as geminin staining, representative images (*left*) and quantification of BRCA1 mean ± S.E.M. foci geminin-positive cells.

(**E**) MDA-MB-436 tumor xenografts expressing mCherry, BRCA1 wild-type and BRCA1-Δ11q were treated with vehicle (black lines), rucaparib (green lines) or cisplatin (red lines) and tumor growth measured, lines represent individual tumors and mice ($n = 5$).

(**F**) Individual tumor volumes at day 30 are shown.

(**G**) Kaplan-Meier survival analyses for mice described in (E).

(**H**) Mice were treated as in (E) for 4 days, tumors were assessed for γ-H2AX and Ki67 staining by IHC. Representative images, scale bars show 50 μM. Mean ± S.E.M quantification of staining intensities. **P* < 0.05.

Figure 5. BRCA1 exon 11 mutations and patient survival.

(**A**) Kaplan-Meier estimates of cumulative survival according to *BRCA1* mutation group of serous ovarian cancer patients (see Supplementary Tables S3 and S4).

(**B**) Primary breast and ovarian cancer patient tumors (unrelated to studies described in (A) were subject to qRT-PCR analysis for +11 and Δ11q expression. Values were normalized to a HKG control and expressed as a percentage of the values calculated for MDA-MB-231 cells. **P* < 0.05.

Figure 6. Splicing inhibition sensitizes exon 11 mutant cells to PARPi.

(**A**) MDA-MB-231, UWB1.289 and SUM149PT cells were transfected with scrambled (Sc) or FOX2#1 and FOX2#2 siRNA and *FOX2*, *POLR2F*, +11 and Δ11q *BRCA1* isoform mRNA levels measured by qRT-PCR. Values were normalized to *POLR2F* HKG expression and expressed as a percentage of MDA-MB-231 cells.

(**B**) Cells treated as in (A) were subject to Western blotting.

(**C**) Cells treated as in (A) were subject to 3 day rucaparib and cisplatin exposure and reseeded for colony formation. Mean±S.E.M. LC50 values are shown.

(**D**) 293T cells were transfected with BRCA1 minigene reporter constructs as in Fig. 1D and Supplementary Fig. S3, with FOX2 binding sites mutated (FOX). BRCA1-Δ11q-

reporter construct mRNA and protein expression was measured by RT-PCR (*left*) and Western blot (*right*), respectively.

(**E**) MDA-MB-231 and UWB1.289 cells incubated with Pl-B (10 nM) and mRNA levels measured by qRT-PCR. Values were expressed as a percentage of vehicle treated MDA-MB-231 cells or UWB1.289 cells.

(**F**) Cells were treated with increasing concentrations of Pl-B and subject to Western blotting.

(**G**) Cells were treated with vehicle (-) or Pl-B (+) (1.25 nM) and either vehicle or rucaparib (100 nM) for 72 hours and reseeded for colony formation assay; mean ± S.E.M. colony formation of rucaparib treated cells calculated as a percentage of vehicle treated cells.

(**H**) SUM149PT cells engineered to ectopically express GFP or BRCA1-Δ11q were treated as in (G) and assessed for colony formation. Western blot (*left*) and mean±S.E.M. colony formation of rucaparib treated cells, calculated as a percentage of vehicle treated cells (*right*). $*P < 0.05$.

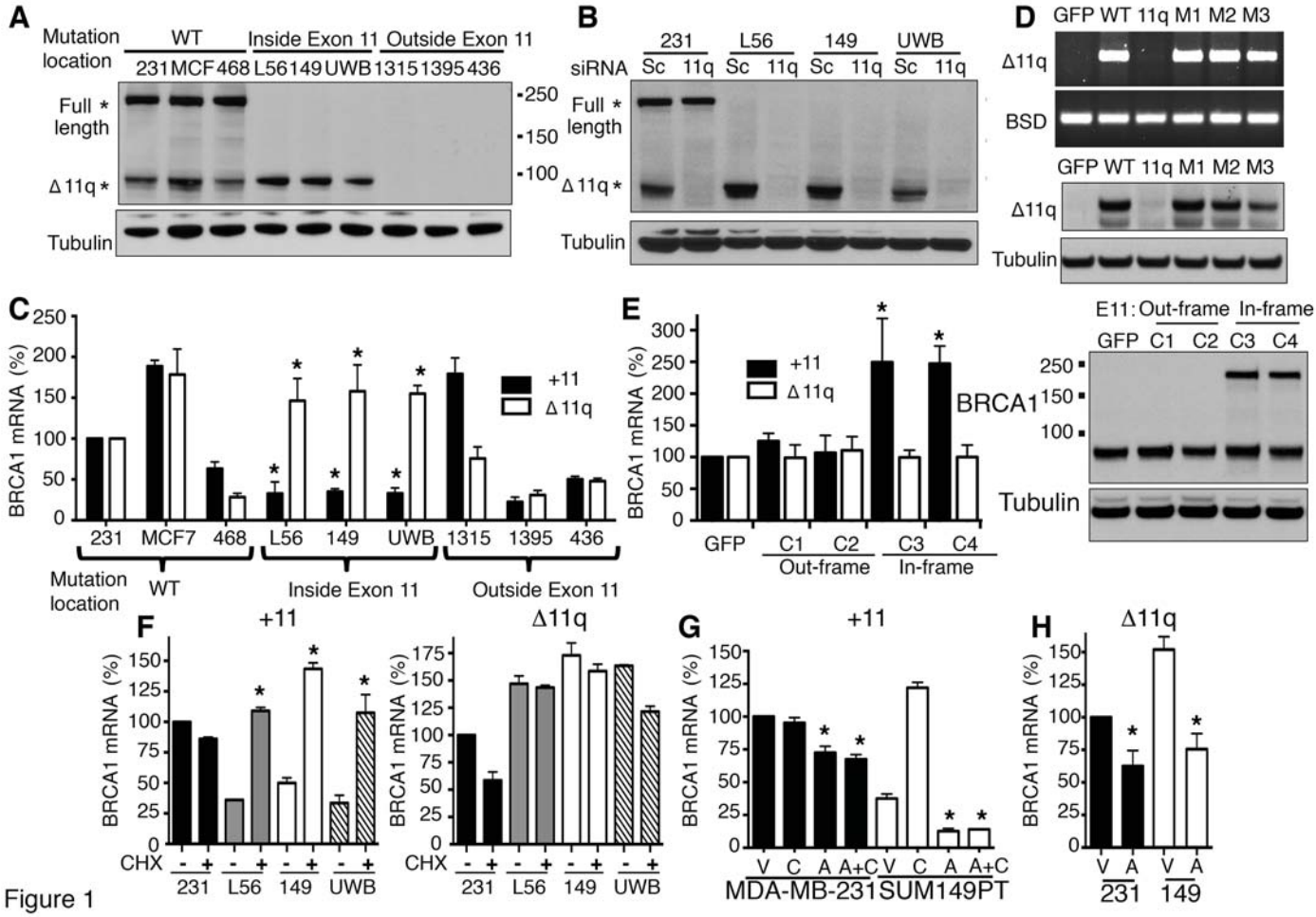
A
Mutation location
WT
Inside Exon 11
Outside Exon 11
231 MCF 468 L56 149 UWB 1315 1395 436
Full length *
Δ11q *
Tubulin
250
150
100
B
231
L56
149
UWB
siRNA
Sc 11q Sc 11q Sc 11q Sc 11q
Full length *
Δ11q *
Tubulin
D
GFP WT 11q M1 M2 M3
Δ11q
BSD
GFP WT 11q M1 M2 M3
Δ11q
Tubulin
C
BRCA1 mRNA (%)
+11
Δ11q
231 MCF7 468 L56 149 UWB 1315 1395 436
Mutation location
WT
Inside Exon 11
Outside Exon 11
E
BRCA1 mRNA (%)
+11
Δ11q
GFP C1 C2 C3 C4
Out-frame
In-frame
E11: Out-frame In-frame
GFP C1 C2 C3 C4
BRCA1
Tubulin
F
+11
Δ11q
BRCA1 mRNA (%)
CHX - + - + - + - +
231 L56 149 UWB
G
+11
BRCA1 mRNA (%)
V C A A+C V C A A+C
MDA-MB-231 SUM149PT
H
Δ11q
BRCA1 mRNA (%)
V A V A
231 149

Figure 1

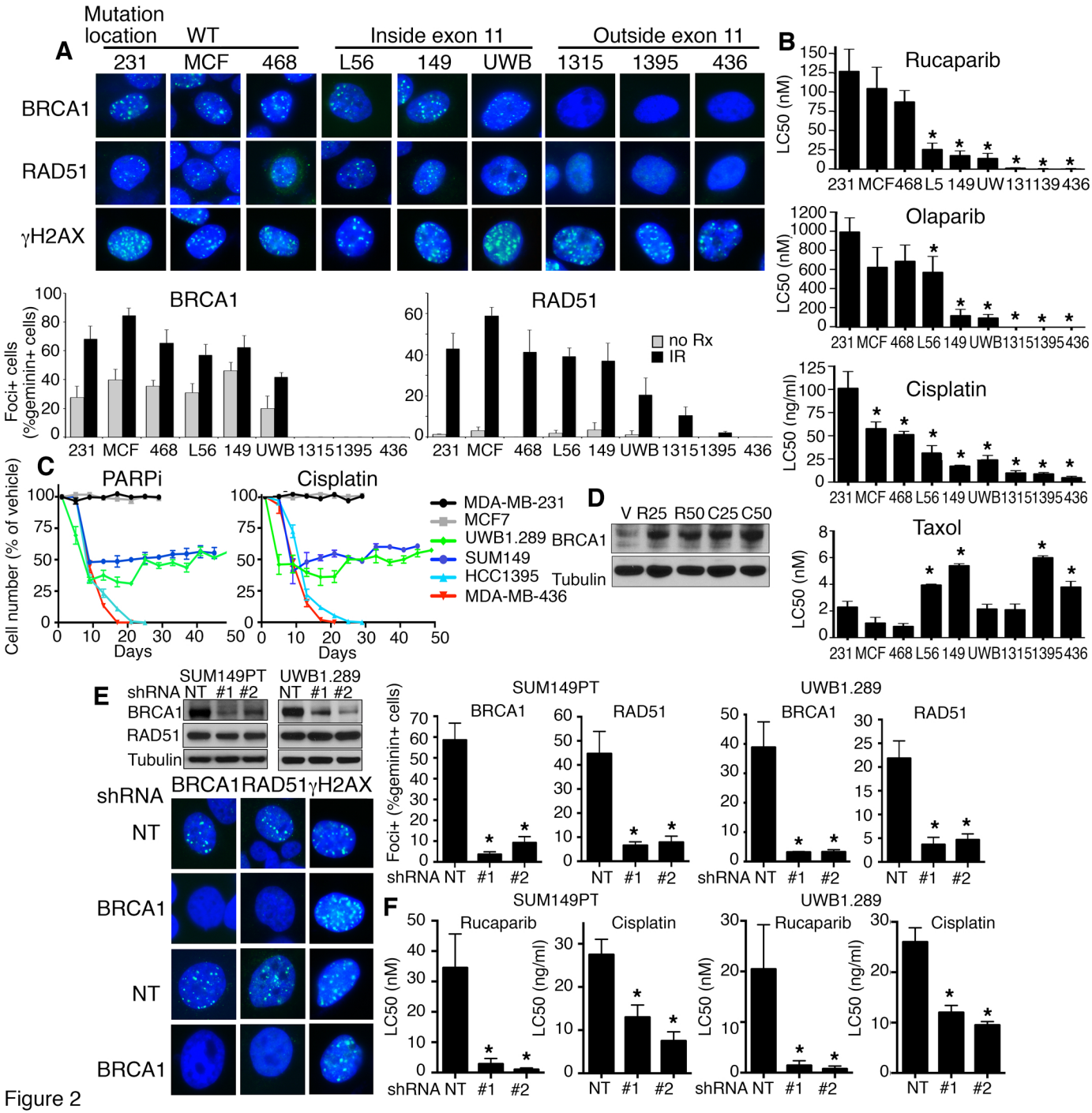
A
Mutation location
WT
Inside exon 11
Outside exon 11
231
MCF
468
L56
149
UWB
1315
1395
436
BRCA1
RAD51
γH2AX
Foci+ cells (%geminin+ cells)
BRCA1
RAD51
no Rx
IR
B
Rucaparib
Olaparib
Cisplatin
Taxol
LC50 (nM)
LC50 (ng/ml)
C
PARPi
Cisplatin
Cell number (% of vehicle)
Days
MDA-MB-231
MCF7
UWB1.289
SUM149
HCC1395
MDA-MB-436
D
V R25 R50 C25 C50
BRCA1
Tubulin
E
SUM149PT
UWB1.289
shRNA NT #1 #2
BRCA1
RAD51
Tubulin
shRNA
BRCA1 RAD51 γH2AX
NT
BRCA1
NT
BRCA1
Foci+ (%geminin+ cells)
F
SUM149PT
UWB1.289
Rucaparib
Cisplatin
LC50 (nM)
LC50 (ng/ml)

Figure 2

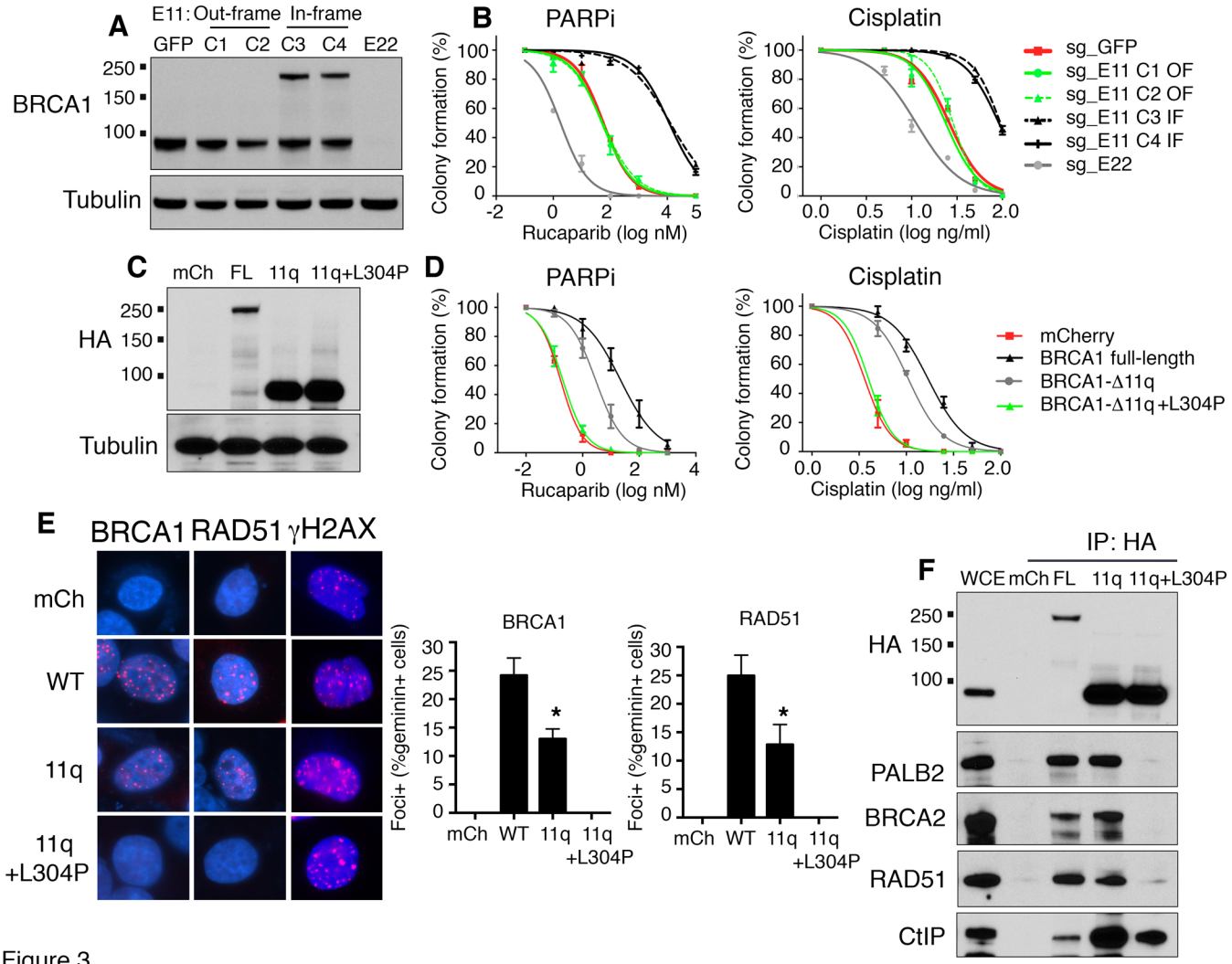
A
E11: Out-frame In-frame
GFP C1 C2 C3 C4 E22
250
150
100
BRCA1
Tubulin
B
PARPi
Colony formation (%)
Rucaparib (log nM)
Cisplatin
Cisplatin (log ng/ml)
sg_GFP
sg_E11 C1 OF
sg_E11 C2 OF
sg_E11 C3 IF
sg_E11 C4 IF
sg_E22
C
mCh FL 11q 11q+L304P
HA
Tubulin
D
PARPi
Cisplatin
mCherry
BRCA1 full-length
BRCA1-Δ11q
BRCA1-Δ11q +L304P
E
BRCA1 RAD51 γH2AX
mCh
WT
11q
11q +L304P
Foci+ (%geminin+ cells)
BRCA1
RAD51
mCh WT 11q 11q +L304P
F
IP: HA
WCE mCh FL 11q 11q+L304P
HA
PALB2
BRCA2
RAD51
CtIP

Figure 3

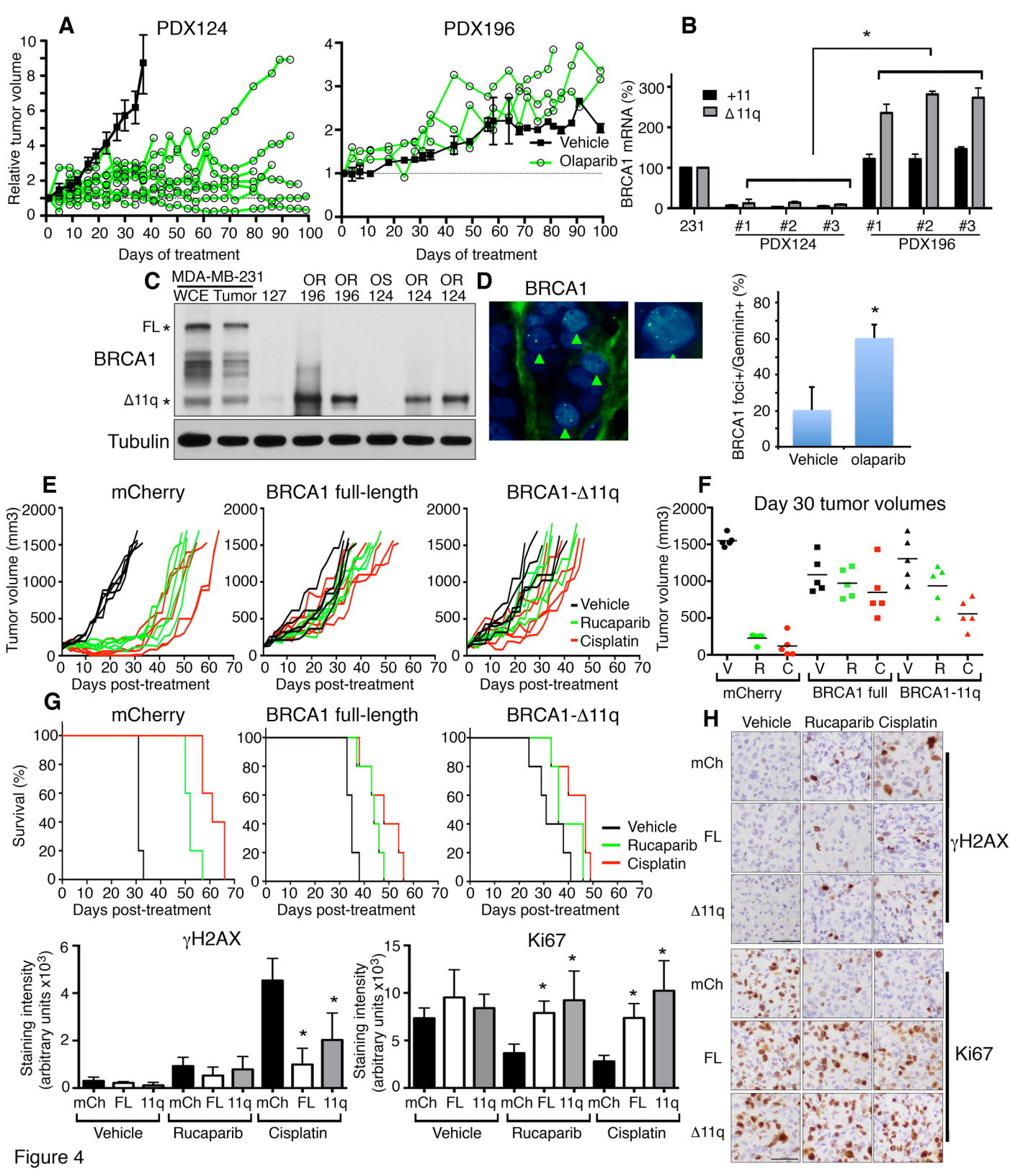
A
PDX124
PDX196
Relative tumor volume
Days of treatment
Vehicle
Olaparib
B
BRCA1 mRNA (%)
+11
Δ11q
231
#1
#2
#3
PDX124
PDX196
C
MDA-MB-231
WCE Tumor 127
OR 196
OR 196
OS 124
OR 124
OR 124
FL *
BRCA1
Δ11q *
Tubulin
D
BRCA1
BRCA1 foci+/Geminin+ (%)
Vehicle
olaparib
E
mCherry
BRCA1 full-length
BRCA1-Δ11q
Tumor volume (mm3)
Days post-treatment
Vehicle
Rucaparib
Cisplatin
F
Day 30 tumor volumes
Tumor volume (mm3)
V
R
C
mCherry
BRCA1 full
BRCA1-11q
G
mCherry
BRCA1 full-length
BRCA1-Δ11q
Survival (%)
Days post-treatment
Vehicle
Rucaparib
Cisplatin
γH2AX
Staining intensity (arbitrary units x10^3)
Ki67
mCh
FL
11q
Vehicle
Rucaparib
Cisplatin
H
Vehicle
Rucaparib
Cisplatin
mCh
FL
Δ11q
γH2AX
Ki67

Figure 4

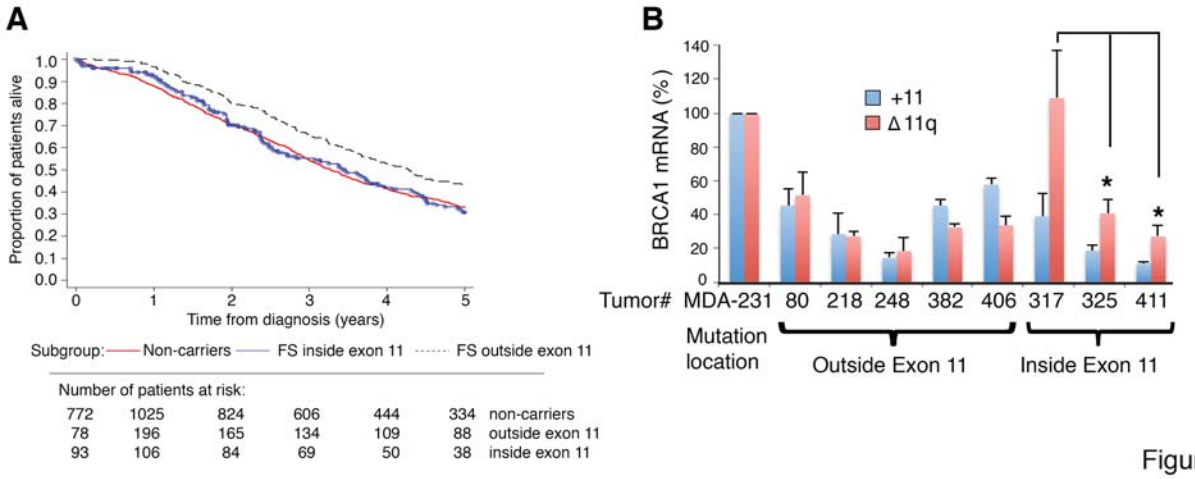
A
Proportion of patients alive
1.0
0.9
0.8
0.7
0.6
0.5
0.4
0.3
0.2
0.1
0.0
0
1
2
3
4
5
Time from diagnosis (years)
Subgroup: Non-carriers FS inside exon 11 FS outside exon 11
Number of patients at risk:
772 1025 824 606 444 334 non-carriers
78 196 165 134 109 88 outside exon 11
93 106 84 69 50 38 inside exon 11
B
BRCA1 mRNA (%)
140
120
100
80
60
40
20
0
+11
Δ11q
*
*
Tumor# MDA-231 80 218 248 382 406 317 325 411
Mutation location
Outside Exon 11
Inside Exon 11

Figure 5

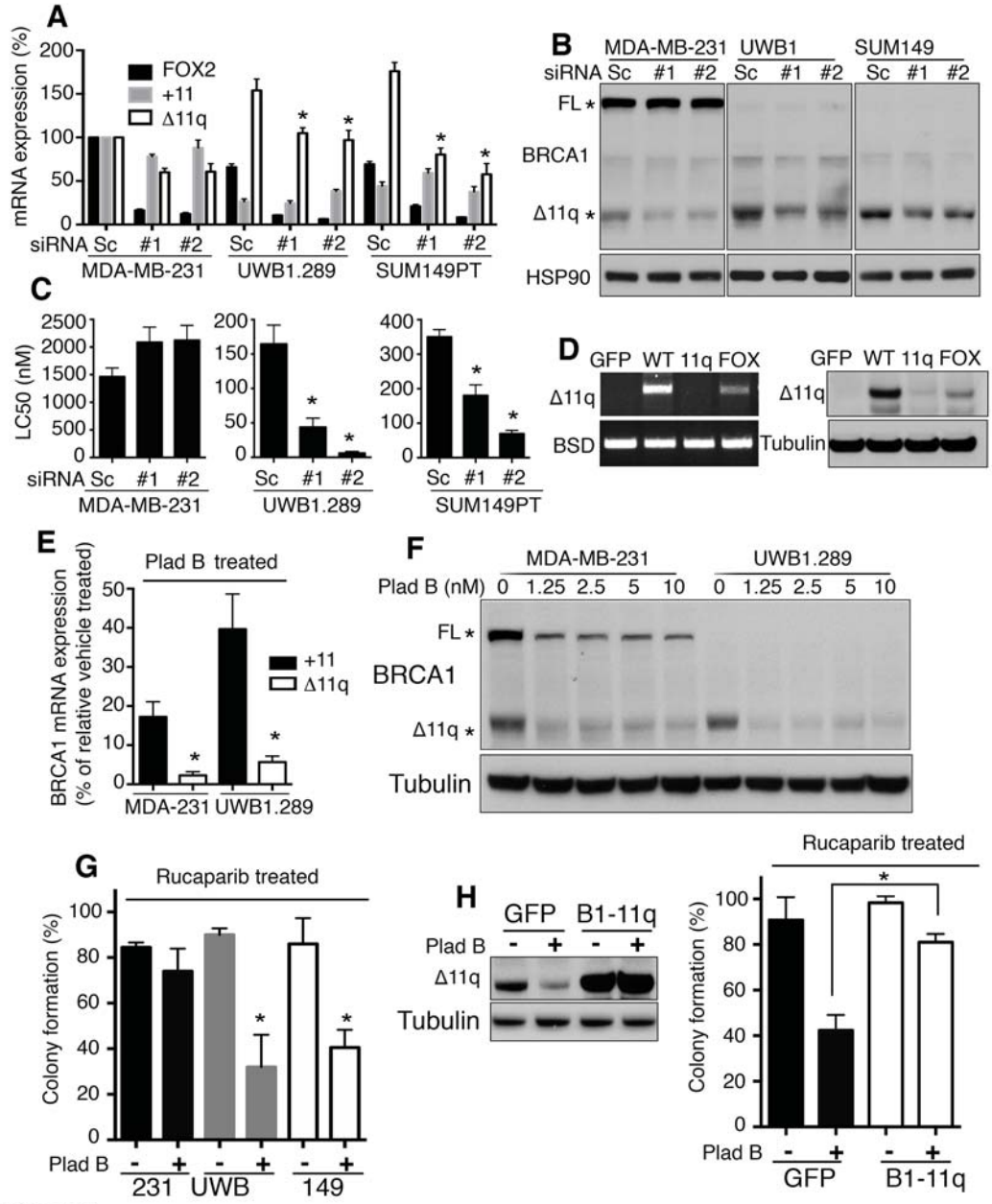
A
mRNA expression (%)
FOX2
+11
Δ11q
siRNA Sc #1 #2 Sc #1 #2 Sc #1 #2
MDA-MB-231
UWB1.289
SUM149PT
B
MDA-MB-231 UWB1 SUM149
siRNA Sc #1 #2 Sc #1 #2 Sc #1 #2
FL *
BRCA1
Δ11q *
HSP90
C
LC50 (nM)
siRNA Sc #1 #2
MDA-MB-231
UWB1.289
SUM149PT
D
GFP WT 11q FOX
Δ11q
BSD
Tubulin
E
Plad B treated
BRCA1 mRNA expression (% of relative vehicle treated)
+11
Δ11q
MDA-231 UWB1.289
F
MDA-MB-231 UWB1.289
Plad B (nM) 0 1.25 2.5 5 10 0 1.25 2.5 5 10
FL *
BRCA1
Δ11q *
Tubulin
G
Rucaparib treated
Colony formation (%)
Plad B - + - + - +
231 UWB 149
H
GFP B1-11q
Plad B - + - +
Δ11q
Tubulin
Rucaparib treated
Colony formation (%)
Plad B - + - +
GFP B1-11q

Figure 6